

# Robust Adaptive Beamforming Based on Fuzzy Cerebellar Model Articulation Controller Neural Network

Jiaqiang Yu, Pingqing Fan\*, Cong Li, and Xiaotian Lu

Automotive Engineering College  
Shanghai University of Engineering Science, Shanghai, 201620, China  
a849710627@gmail.com, fanpingqing@163.com, licong@sues.edu.cn, ephgiw@163.com

**Abstract** – To solve the problem of degraded adaptive beamforming performance of smart antenna caused by array steering vector mismatch and array manifold errors, a robust beamforming algorithm based on Fuzzy Cerebellar Model Articulation Controller (FCMAC) neural network is proposed. The proposed algorithm is based on explicit modeling of uncertainties in the desired signal array response and a FCMAC neural network. The calculation of the optimal weight vector is viewed as a mapping problem, which can be solved using FCMAC neural network trained with input/output pairs. Our proposed approach provides excellent robustness against some types of mismatches and keeps the mean output array SINR consistently close to the optimal value. Moreover, the FCMAC neural network avoids complex matrix inversion operations and offers fast convergence rate. Simulation results show that the proposed algorithm can significantly enhance the robustness of the beamformer in the presence of array steering vector mismatch and array manifold errors, and the output performance is superior to the current methods.

**Index Terms** – Adaptive beamforming, FCMAC, neural network, robustness, steering vector mismatch.

## I. INTRODUCTION

Adaptive beamforming is a technique used to receive desired signals and suppress interferences by adjusting the weight vectors of arrays adaptively. It is widely applied in various fields, including wireless communication, radar and sonar [1,2].

After the publication of the standard Capon beamformer [3], various robust adaptive beamformers have been developed based on different criteria, such as diagonal loading [4], Worst-Case performance optimal [5], Least Mean Squares (LMS) [6] and linear constraints [7]. To alleviate the performance degradation of the traditional adaptive beamformers caused by steering vector mismatch and array manifold errors, some robust adaptive beamforming based on steering vector estimation have been proposed in recent years [8-10]. To further increase the performance, several methods based on

interference-plus-noise covariance matrix reconstruction were proposed after, including sparse reconstruction [11,12], spatial power spectrum sampling [13], annulus uncertainty set [14], subspace-based reconstruction [15]. Li et al. proposed a null broadening beamforming approach based on covariance matrix expansion to improve the performance of antenna array beamforming in the case of jammer motion [16].

Neural network is a nonlinear adaptive dynamical system and provides a new idea for adaptive beamforming algorithms [17-20]. Sallomi and Ahmed used artificial Feed Forward Neural Network (FFNN) for smart antenna adaptive beamforming [21]. Higuchi derive a frame-by-frame update rule for a mask-based minimum variance distortion-less response (MVDR) beamformer, which enables us to obtain enhanced signals without a long delay by combining it with unidirectional recurrent neural network-based mask estimation [22]. It is well known that the FCMAC is a special feed-forward neural network based on local approximation that can be adapted to solve the multidimensional nonlinear fitting problem [23-25]. Compared to global approximation methods such as BP neural network, CMAC has attractive features of special architecture, fast learning capability and a certain degree of generalization.

In this paper, we present an improved robust adaptive beamforming (RAB) algorithm based on FCMAC neural network. Firstly, we explicitly express the uncertainty of the expected signal array response based on the worst-case performance optimization, so the constrained optimization problem is transformed into a convex optimization problem. Secondly, the calculation of optimal weight is treated as a mapping problem by using the FCMAC neural network. The proposed RAB algorithm offers fast convergence rate and enhances the array system performance under non-ideal conditions. Lastly, several examples are presented to demonstrate the performances of the proposed robust beamforming algorithm.

## II. SMART ANTENNA SYSTEM

The smart antenna system is an array of antennas that terminated into a smart signal processing unit to

make the transmission and reception of antenna system in an adaptive, spatially sensitive manner. Smart antennas are able to separate signals from multiple sources and enhance the performance of cellular communications systems. The adaptive algorithms that used by the digital signal processing (DSP) unit of antenna array system give the ability and the Intelligence of smart antenna systems. The block diagram of a smart antenna system with  $M$  elements is shown in Fig. 1.

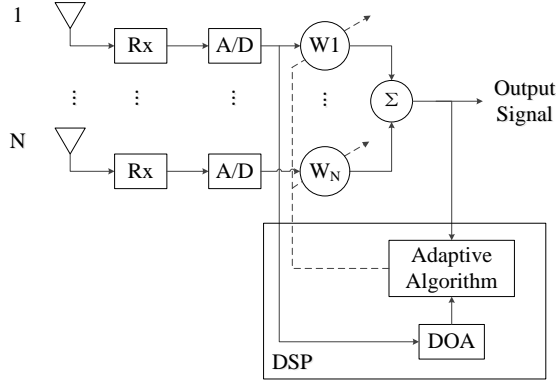


Fig. 1. Block diagram of a smart antenna system.

Where, A/D refer to the analog to digital convertor,  $w_1 \sim w_M$  are the weights of an antenna array that obtained by the adaptive algorithm of DSP unit. DOA refer to the direction of arrival estimator that estimate the angle of arrival of the received signals.

### III. SIGNAL MODEL

Adaptive Beamforming is an intelligence signal processing technique in which the received signals by each element of the antenna array are multiplied by complex weight vectors to adapt the magnitude and phase of the received signals in order to direct maximum radiation in the direction of desired users and nulling interferer sources. The signals received by different elements of an antenna array combined to form a single output. Classically, this is achieved by decreasing the mean square error (MSE) between the desired output and actual array output. Figure 2 shows the block diagram of adaptive beamformer.

In this part, we consider a uniform linear array consisting of  $N$  isotropic antenna elements spaced by the distance  $d$ . Assume that there are  $P$  far-field narrowband signals impinging on the array. At the time  $t$ , the array observation can be written as:

$\mathbf{X}(t) = \mathbf{S}(t) + \mathbf{i}(t) + \mathbf{n}(t) = s(t)\mathbf{a} + \mathbf{i}(t) + \mathbf{n}(t)$ , (1) where  $\mathbf{X}(t) = [x_1(t), x_2(t), \dots, x_N(t)]^T$ , it is the complex vector of array observations,  $\mathbf{S}(t)$ ,  $\mathbf{i}(t)$ ,  $\mathbf{n}(t)$  denote the statistically independent components of the desired signal, interference, and noise, respectively.  $s(t)$  is waveform of the desired signal,  $\mathbf{a}$  is desired signal

steering vector. The output of a narrowband beamformer at time  $t$  is given by:

$$y(t) = \sum_{i=1}^N x_i(t)w_i = \mathbf{W}^H \mathbf{X}(t), \quad (2)$$

where  $\mathbf{W} = [w_1, w_2, \dots, w_N]^H$  represents complex weight vector.  $(\cdot)^T$  and  $(\cdot)^H$  denote the transpose and Hermitian transpose, respectively. The out signal-to-interference-plus-noise ratio (SINR) of the beamformer has the following form:

$$SINR = \frac{\sigma_s^2 |\mathbf{W}^H \mathbf{a}|^2}{\mathbf{W}^H \mathbf{R}_{i+n} \mathbf{W}}, \quad (3)$$

where  $\sigma_s^2$  denotes the power of the desired signal,  $\mathbf{R}_{i+n}$  denotes interference-plus-noise covariance matrix. According to the minimum variance distortionless response (MVDR) principles, the maximization of SINR (3) is equivalent to minimization interference plus noise power:

$$\min_{\mathbf{W}} \mathbf{W}^H \mathbf{R}_{i+n} \mathbf{W} \quad \text{subject to} \quad \mathbf{W}^H \mathbf{a} = 1. \quad (4)$$

From (4), the well-known solution can be obtained by the following optimal weight vector:

$$\mathbf{W}_{opt} = \frac{\mathbf{R}_{i+n}^{-1} \mathbf{a}}{\mathbf{a}^H \mathbf{R}_{i+n}^{-1} \mathbf{a}}. \quad (5)$$

Inserting (5) into (3), the optimal SINR is given by:

$$SINR_{opt} = \sigma_s^2 \mathbf{a}^H \mathbf{R}_{i+n}^{-1} \mathbf{a}. \quad (6)$$

However, the exact  $\mathbf{R}_{i+n}$  is unavailable in practical applications, it requires an infinite number of pure snapshots data without the desired signal. Therefore, it is usually replaced by sample covariance matrix  $\hat{\mathbf{R}} = (1/K) \sum_{i=1}^K \mathbf{X}(i)\mathbf{X}^H(i)$ , where  $K$  is the number of snapshots. The resultant beamforming algorithm is commonly referred to as the sample matrix inversion (SMI) algorithm:

$$\mathbf{W}_{SMI} = \frac{\hat{\mathbf{R}}^{-1} \mathbf{a}}{\mathbf{a}^H \hat{\mathbf{R}}^{-1} \mathbf{a}}. \quad (7)$$

When the number of snapshots  $K$  is small, the large gap between the known  $\hat{\mathbf{R}}$  and  $\mathbf{R}_{i+n}$  can significantly affect the performance of the SMI algorithm, especially when there is a desired signal in the training samples. For this reason, this paper proposes a new robust adaptive beamforming algorithm.

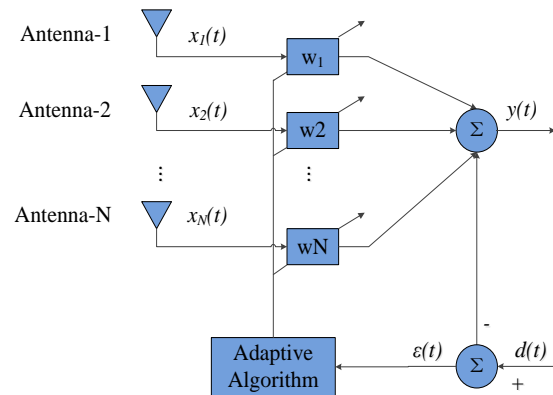


Fig. 2. Adaptive beamformer.

## IV. ROBUST ADAPTIVE BEAMFORMING BASED ON FCMAC NEURAL NETWORK

### A. Robust adaptive beamforming

In practical applications, we assume that the norm of the steering vector distortion  $\Delta$  can be bounded by some known constant  $\varepsilon > 0$ :

$$\|\Delta\| \leq \varepsilon. \quad (8)$$

According to [26], we can rewrite the optimization problem (4) as follows:

$$\begin{aligned} & \min_{\mathbf{W}} \mathbf{W}^H \mathbf{R} \mathbf{W} \\ & \text{subject to } \mathbf{W}^H \mathbf{a} = \varepsilon \|\mathbf{W}\| + 1, \end{aligned} \quad (9)$$

where  $\mathbf{R} = E[\mathbf{X}(i)\mathbf{X}^H(i)]$  denotes theoretical covariance matrix of array out vector.

According to [27], considering the worst-case mismatch, a meaningful express of (9) can be written as:

$$\begin{aligned} & \min_{\mathbf{W}} \max_{\Delta_1 \leq \gamma} \mathbf{W}^H (\mathbf{R} + \Delta_1) \mathbf{W} \\ & \text{subject to } \mathbf{W}^H \mathbf{a} = \varepsilon \|\mathbf{W}\| + 1, \end{aligned} \quad (10)$$

where the matrix  $\Delta_1$  takes all possible steering vector distortions into account, such as nonstationarity of the data, small training samples and quantization errors, etc. This situation is also referred to the worst-case optimization problem. To solve the (10), we can first solve the following optimization problem:

$$\begin{aligned} & \max_{\Delta_1} \mathbf{W}^H (\mathbf{R} + \Delta_1) \mathbf{W} \\ & \text{subject to } \|\Delta_1\| \leq \gamma. \end{aligned} \quad (11)$$

Rewriting this problem as:

$$\begin{aligned} & \min_{\Delta_1} -\mathbf{W}^H (\mathbf{R} + \Delta_1) \mathbf{W} \\ & \text{subject to } \|\Delta_1\| \leq \gamma. \end{aligned} \quad (12)$$

From the linearity of this objective function, the inequality constraint in (12) can be replaced by the equality constrain:

$$\|\Delta_1\| = \gamma. \quad (13)$$

We can use the Lagrange multiplier method to solve the (12) optimization problem:

$$\Psi(\Delta_1, \lambda) = -\mathbf{W}^H (\mathbf{R} + \Delta_1) \mathbf{W} + \lambda (\|\Delta_1\|^2 - \gamma^2). \quad (14)$$

Calculating the gradient of (14) and equating it to zero yields:

$$\Delta_1 = \frac{\mathbf{w}\mathbf{w}^H}{2\lambda}. \quad (15)$$

Combining (15) and (13), we can obtain:

$$\lambda = \frac{\|\mathbf{w}\|^2}{2\gamma}, \quad (16)$$

$$\Delta_1 = \gamma \frac{\mathbf{w}\mathbf{w}^H}{\|\mathbf{w}\|^2}. \quad (17)$$

Therefore, we can figure out the (11) by (17). Correspondingly, (10) can be written as:

$$\begin{aligned} & \min_{\mathbf{W}} \mathbf{W}^H (\mathbf{R} + \gamma \mathbf{I}) \mathbf{W} \\ & \text{subject to } \mathbf{W}^H \mathbf{a} = \varepsilon \|\mathbf{W}\| + 1. \end{aligned} \quad (18)$$

In the same way, we construct Lagrange function:

$$\begin{aligned} L(\mathbf{W}, \lambda) = & \mathbf{W}^H (\mathbf{R} + \gamma \mathbf{I}) \mathbf{W} + \lambda (\varepsilon^2 \mathbf{W}^H \mathbf{W} - \mathbf{1} - \\ & \mathbf{W}^H \mathbf{a} \mathbf{a}^H \mathbf{W} + \mathbf{W}^H \mathbf{a} + \mathbf{a}^H \mathbf{W}). \end{aligned} \quad (19)$$

Differentiating  $L(\mathbf{W}, \lambda)$  with respect to  $\mathbf{W}$ ,  $\lambda$  and setting these partial derivatives to zero, we can obtain respectively:

$$(\mathbf{R}_{DL} + \lambda \mathbf{G}) \mathbf{W} = -\lambda \mathbf{a}, \quad (20)$$

$$\mathbf{W}^H \mathbf{G} \mathbf{W} \mathbf{W}^H \mathbf{a} + \mathbf{a}^H \mathbf{W} = 1, \quad (21)$$

where matrices  $\mathbf{R}_{DL}$  and  $\mathbf{G}$  are defined as:

$$\mathbf{R}_{DL} = \mathbf{R} + \gamma \mathbf{I}, \quad (22)$$

$$\mathbf{G} = \varepsilon^2 \mathbf{I} - \mathbf{a} \mathbf{a}^H. \quad (23)$$

According to (20), we can obtain:

$$\mathbf{W}_{RAB} = -\lambda (\mathbf{R}_{DL} + \lambda \mathbf{G})^{-1} \mathbf{a}. \quad (24)$$

Inserting this to (21) yields:

$$\begin{aligned} f(\lambda) = & \lambda^2 \mathbf{a}^H (\mathbf{R}_{DL} + \lambda \mathbf{G})^{-1} \mathbf{G} (\mathbf{R}_{DL} + \lambda \mathbf{G})^{-1} \mathbf{a} \\ & - 2\lambda \mathbf{a}^H (\mathbf{R}_{DL} + \lambda \mathbf{G})^{-1} \mathbf{a} - 1 = 0. \end{aligned} \quad (25)$$

To solve (25), we can use the method of matrix eigenvalue decomposition:

$$f(\lambda) = \lambda^2 \sum_{i=1}^n \frac{g_i^2 r_i}{(1+\lambda r_i)^2} - 2\lambda \sum_{i=1}^n \frac{g_i^2}{1+\lambda r_i} - 1, \quad (26)$$

where  $g_i$  and  $r_i$  denotes the generalized eigenvalue of matrices  $\mathbf{G}$  and  $\mathbf{R}_{DL}$ .

The above robust adaptive beamforming algorithm considers the problem of steering vector mismatch. Some methods are proposed that using the variable diagonal loading factor to calculate the weight of the beamformer [28]. In these papers, they make the diagonal loading factor equal to the standard deviation of the diagonal elements of the covariance matrix, which adapts to changes in the number of snapshots and does not require any prior information:

$$\gamma = \text{std}(\text{diag}(\mathbf{R})). \quad (27)$$

Since the above equation (24) involves matrix inversion, it is not practical for real-time implementation. Therefore, this paper uses the FCMAC neural network to calculate the optimal weight of a uniform linear antenna array. The trained FCMAC neural network model can convert the calculation of the optimal weight vector into a mapping problem. Furthermore, the FCMAC neural network with local approximation and good generalization performance can provide fast convergence rate.

### B. The cerebellar model articulation controller neural network

The structure of CMAC neural network is shown in Fig. 3, which contains Input Space (X), Association Memory Space (A), Physical Space (W) and Output Space (Y). After being quantified, each vector in the Input Space is mapped to the Association Memory Space and activates  $N_L$  storage units, which is corresponding to  $N_L$  weights stored in the Physical Space. The output  $y_i$  of CMAC neural network equals to the sum of these  $N_L$  weights. For an input sample, the desired output value can always be achieved by adjusting the weight.

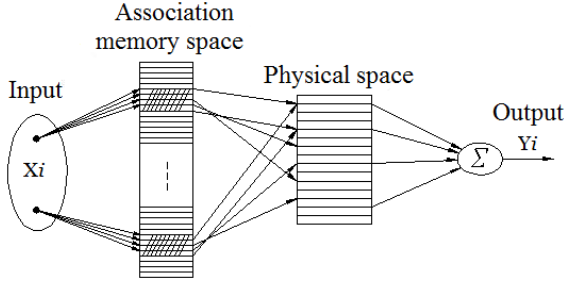


Fig. 3. The structure of CMAC neural network.

In the Association Memory Space, the input for each dimension is further divided into  $p$  layers and  $q$  blocks, and the number of equal-divided slices of each dimension is  $[p(q-1)+1]$ . The weight equals to the accumulation of the active blocks at each layer, so the number of possible weights is  $(p \cdot q^n)$ , where  $n$  is the input dimension. As shown in Fig. 4, assume that the two-dimensional input CMAC neural network is divided into 4 layers and 2 blocks, so the number of equal-divided slices of each dimension equals to 5, the number of possible weights equals to 16, but the number of weights  $N_L$  activated by each input variable  $X_i$  equals to 4, whose index are Bb, Dd, Ff and Gg. It can be seen that the CMAC neural network have similar outputs for similar inputs, which means that it possesses strong ability of local generation.

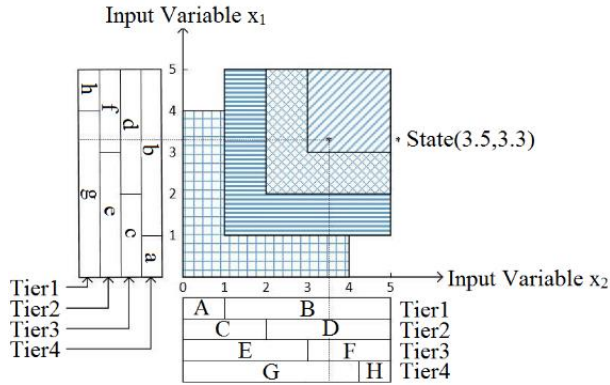


Fig. 4. The mapping principle of Association Memory Space.

The main working principle of CMAC neural network is divided into three mapping processes.

### 1) Conceptual mapping ( $X \rightarrow A$ )

The input of CMAC can be regarded as a multi-dimension vector ( $X$ ). It can be quantized first and then mapped to the corresponding activated units in Association Memory Space ( $A$ ). The quantization algorithm is given by:

$$\bar{x}_i = \frac{x_i - x_{\min}}{x_{\max} - x_{\min}} \cdot M, \quad (28)$$

where  $M = p(q-1) + 1$ . The quantized interval for each input variable overlaps in each quantization layer, and on any two units are exactly the same. There is a step  $\Delta q$  in every two quantization layers. When the input signal falls into a quantized interval, the corresponding memory cell is activated. The  $\text{ceil}()$  function and  $\text{floor}()$  function can be used to encode the address of the activated memory cell according to equation (31):

$$a_i = \begin{cases} 0 & \text{if } x_i < x_{\min} + O_j \\ \text{ceil}\left(\frac{\bar{x}_i - x_{\min} - O_j}{S_C}\right) & \text{otherwise} \\ \text{else} & \end{cases}$$

where  $O_j = \Delta q \times N_j$  ( $N_j = 0, 1, \dots, N_L$ ) represents the offset of each quantization layer,  $S_C$  is the size of memory cell. Therefore, the input vector  $X$  is mapped to a relevant binary address vector.

### 2) Address calculation ( $A \rightarrow W$ )

The units in Physical Space ( $W$ ) store the weight values and the address units in Association Memory Space ( $A$ ) can be mapped to the corresponding weight units in  $W$  by Hash-coding.

### 3) Output mapping ( $W \rightarrow Y$ )

This mapping relation is used to calculate the output of CMAC, which means that add all the weight values of the activated units in  $W$  and regard the result as the final output.

## C. The fuzzy cerebellar model articulation controller neural network

As shown in Fig. 5, by introducing the fuzzy inference rules into a CMAC, this paper uses a more generalized network, called FCMAC. The Gaussian function is adopted here as the fuzzy membership function, which can be represented as:

$$G_j = \exp\left(-\frac{(\bar{x}_j - \mu_j)^2}{\delta_j^2}\right) \quad (j = 1, 2, \dots, N_L), \quad (30)$$

where  $\delta_j$  represents  $j$ th Gaussian function variance of memory cells,  $\mu_j$  represents  $j$ th Gaussian function expectation of memory cells. The output of FCMAC can be expressed as:

$$y_i = \sum_{j=1}^{N_L} w_j G_j \quad i = 1, 2, \dots, N. \quad (31)$$

The following algorithms are used to adjust the network weights

$$w_j(t) = w_j(t-1) + \frac{\alpha}{N_L} G_j (\bar{y}_s - \sum_{j=1}^{N_L} G_j w_j(t-1)), \quad j = 1, 2, \dots, N_L, \quad (32)$$

where  $\alpha$  denotes the learning rate,  $\bar{y}_s$  is the desired output and  $\sum_{j=1}^{N_L} G_j w_j(t-1)$  is the actual output, only the activated weights are updated.

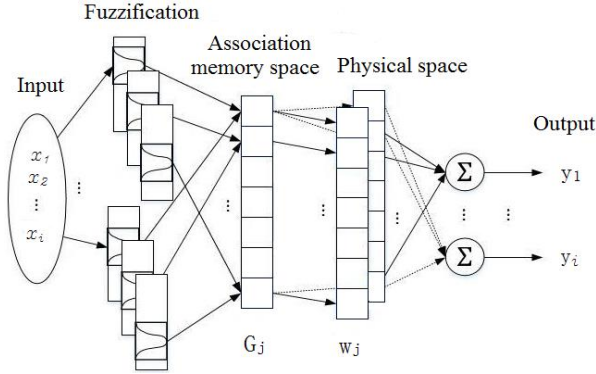


Fig. 5. The structure of FCMAC neural network.

#### D. Training data generation and neural network learning

Firstly, the normalized samples are obtained according to the signal's different incidence angles  $\theta$  and SNR parameters:

$$X_n = X / \|X\|. \quad (33)$$

Then the correlation matrix of the incoming signals that received by  $N$  elements of antenna array system are generated as follows:

$$\mathbf{R} = \frac{1}{N} \sum_{n=1}^N X_n (X_n)^H = \begin{bmatrix} R_{11} & R_{12} & \dots & R_{1N} \\ R_{21} & R_{22} & \dots & R_{2N} \\ \dots & \dots & \dots & \dots \\ R_{N1} & R_{N2} & \dots & R_{NN} \end{bmatrix}, \quad (34)$$

where  $(\cdot)^H$  refers to conjugate transpose of matrix. Then the first row of the correlation matrix  $\mathbf{R}$  is used as the input of neural network since it contains adequate information of the received signal:

$$\mathbf{Z} = [R_{11} \ R_{12} \ \dots \ R_{1N}]. \quad (35)$$

Due to the fact that the neural network does not operate with complex number, the real and imaginary part of each element in  $\mathbf{Z}$  vector is taken, which means the dimension of  $\mathbf{Z}$  vector will be twice ( $1 \times 2N$ ). The antenna element optimal weight vector  $\mathbf{W}_{\text{RAB}}$  calculated from equation (24) is used as the target output of the neural network, which can direct the main beam of radiation pattern toward desired signal and place nulls at interference directions in optimal form.

Assume that the angle  $\theta$  of incoming signals range from  $-90^\circ$  to  $90^\circ$  and the interval is  $1^\circ$ , then 181 sets of training sample data are generated to train the FCMAC network. The weights are iteratively corrected by using equation (32). The neural network training process is shown in Fig. 6.

As shown in Fig. 6, the FCMAC has established an approximation of the desired input-output mapping after the training is completed. In the performance phase, the FCMAC produces outputs to previously unseen inputs by interpolating between the inputs used in the training phase.

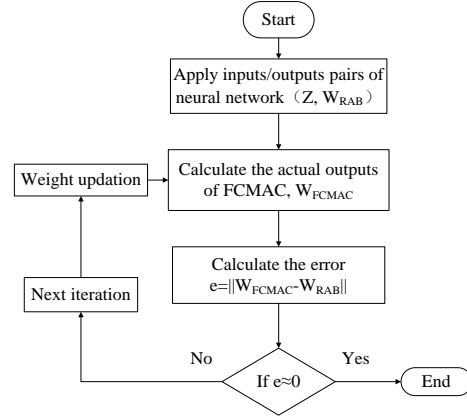


Fig. 6. Training process of FCMAC.

## V. SIMULATION RESULTS

To examine the performance of the proposed algorithm, simulations were performed on a uniform linear array with  $N=10$  sensors and inter-element spacing is half the wavelength of the desired signal. The parameters of the FCMAC network are  $p=4$ ,  $q=3$ , and the learning constant  $\alpha$  is 0.05. The presumed desired signal direction is set to  $0^\circ$ , interference directions are set to  $40^\circ$ , and the interference-to-noise-ratio (INR) equals to 35 dB. The additive noise is modeled as complex circularly symmetric Gaussian zero-mean spatially and temporally white process. The worst-performing optimal algorithm steering vector uncertainty set  $\varepsilon = 3$ . For each scenario, the average of 50 independent runs is used to plot each simulation point. The optimal SINR is also plotted for reference.

#### A. Example 1: Array beam patterns of the algorithms

In the example, the scenario with the signal look direction mismatch is considered and compared to the ideal case. We assume that both the presumed and actual signal spatial signatures are plane waves impinging from the DOAs  $0^\circ$  and  $3^\circ$  respectively. This corresponds to a  $3^\circ$  mismatch in the signal look direction. The input signal-noise-ratio (SNR) is set to 15dB and the number of snapshots  $K$  is set to 100. Figure 7 and Fig. 8 display the beam patterns of the different methods for the no-mismatch case and for a  $3^\circ$  mismatch respectively.

From Fig. 7, we can note that the FCMAC-RAB algorithm can direct the main beam of radiation pattern toward desired signal and place nulls at interference directions. Compared to the SMI, LSMI and LMS algorithm, the proposed beamformer have lower sidelobes and deeper null, which can prevent significant performance degradation in the case of unexpected interfering signals.

From Fig. 8, we note that the SMI and LMS algorithm does not have robustness to the steering vector mismatch, and may mistake the desired signal as interference. Although the LSMI algorithm has certain

stability to the steering vector mismatch, it is at the cost of decreasing the interference nulling-depth. The FCMAC-RAB algorithm can maintain a good beamforming capability and sufficient null-depth in the presence of interference. The corresponding amplitude distribution obtained by four different algorithms are given in Table 1. From Table 1, we can note that FCMAC-RAB algorithm is lower than LMS algorithm 8.7 dB in interference inhibition gain and 0.6 dB in sidelobe gain.

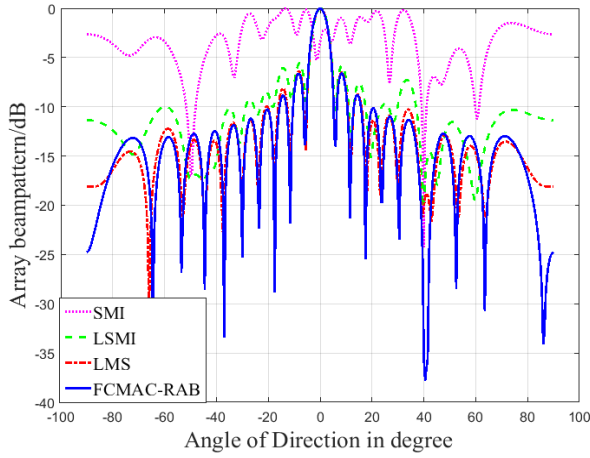


Fig. 7. Directional pattern of each beamforming algorithm (no mismatch).

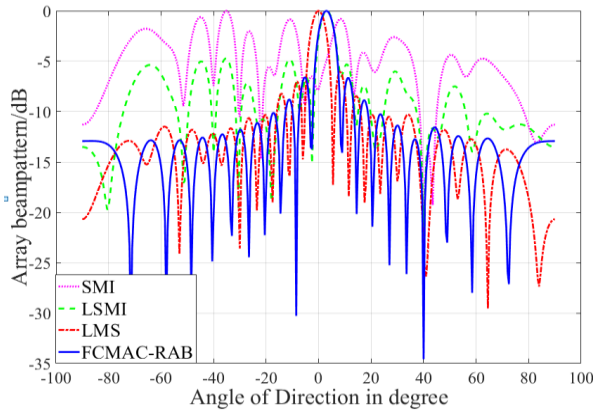


Fig. 8. Directional pattern of each beamforming algorithm (a 3° mismatch).

Table 1: Amplitude distribution obtained by different algorithms

Algorithm	SMI	LSMI	LMS	FCMAC
Sidelobe gain/dB	-4.7	-5.3	-6.1	-6.7
Interference gain/dB	-17.2	-17.7	-25.9	-34.6

**B. Example 2: Robustness analysis of the algorithms**

In this example, the output SINR of the beamformers versus input SNR and the number of snapshots K with the array pointing error are considered respectively.

Firstly, the number of snapshots K is set to 100 and the expected signal SNR varies from -10 to 30 dB. Comparing the output SINR of each algorithm with the expected signal SNR, the simulation results are shown in Fig. 9. Secondly, the expected signal SNR is set to 20 dB, the number of snapshots K is changed from 1 to 100. The relationship between the SINR of each algorithm and K is compared. The simulation results are shown in Fig. 10.

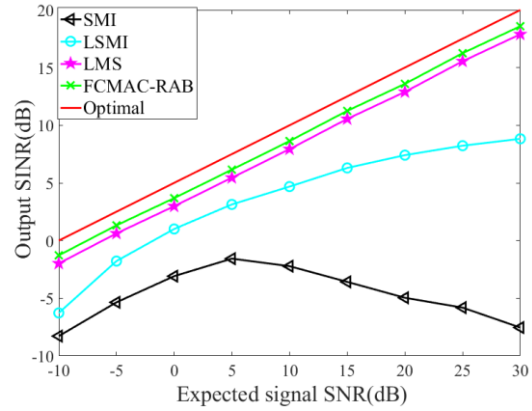


Fig. 9. The relationship between the system output SINR and input SNR for fixed K=100.

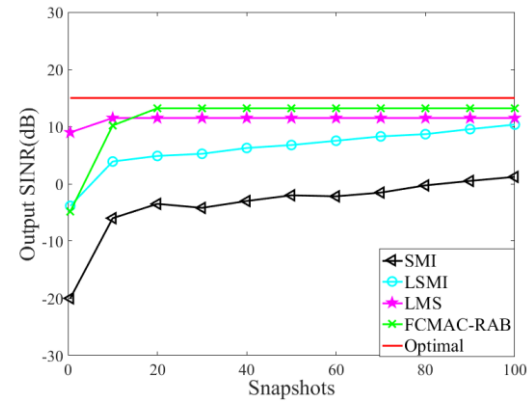


Fig. 10. The relationship between the system output SINR and the snapshots K for fixed SNR=20dB.

It can be observed from Fig. 9 and Fig. 10 that SMI algorithm is very sensitive even to slight mismatches and LSMI algorithm can improve the performance of the SMI algorithm. Obviously, the performance of the FCMAC-RAB algorithm is close to the optimal one at different SNR and K. Additionally, both the SMI and LSMI algorithms show a decrease in performance when the input SNR is high. This is because the algorithm

mistakes the desired signal as an interfering signal when the desired signal SNR is high. Compared with the LMS algorithm, the output performance of FCMAC-RAB algorithm is improved by 1dB. The result demonstrates that the proposed beamforming algorithm present quite bigger output SINR than all the other tested beamformers.

### C. Example 3: Analysis of training performance under different neural networks

In this example, the performance of FCMAC network is compared with the Radial Basis Function (RBF) neural network. The number of trainings is set to 100 times. The other conditions are the same as example1. The simulation results are shown in Fig. 11.

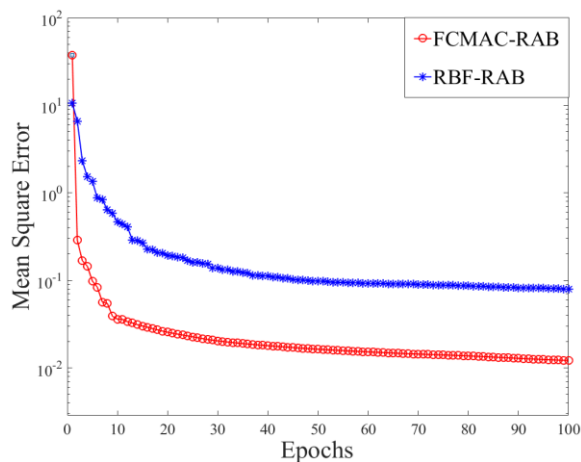


Fig. 11. Convergence of FCMAC and RBF neural network.

As shown in Fig. 11, the best training performance of FCMAC neural network and RBF neural network are [0.0426] at epoch 20 and [0.118] at epoch 30, respectively. From the result, we can infer that FCMAC neural network provides faster convergence rate and smaller error than RBF neural network during training, which proves that FCMAC neural network has the characteristics of local approximation and fast learning speed.

## VI. CONCLUSION

We have introduced a new robust adaptive beamforming algorithm based on FCMAC neural network to improve adaptive beamforming performance of smart antenna. The proposed algorithm is based on explicit modeling of uncertainties in the desired signal array response and a FCMAC neural network. Simulation results demonstrate that the RAB-FCMAC algorithm maintains a good beamforming capability and sufficient null-depth in the presence of interference. Compared to LMS algorithm, the FCMAC-RAB algorithm decreases 8.7 dB in interference inhibition gain and 0.6 dB in sidelobe gain. Furthermore, RAB-FCMAC algorithm

keeps the mean output array SINR consistently close to the optimal value in a wide range of the SNR and the number of snapshots and offers faster convergence rate than RBF neural network.

## ACKNOWLEDGMENT

The authors gratefully acknowledge that this work was partially supported by the Program of National Natural Science Foundation of China under Grant No. 51505275.

## REFERENCES

- [1] W. Li, X. Mao, Z. Zai, and Y. Li, "A low complexity high performance robust adaptive beamforming," *Applied Computational Electromagnetics Society*, vol. 32, no. 5, pp. 441-448, 2017.
- [2] W. M. Jia, W. Jin, S. H. Zhou, and M. L. Yao, "Robust adaptive beamforming based on a new steering vector estimation algorithm," *Signal Processing*, vol. 93, no. 9, pp. 2539-2542, 2013.
- [3] J. Capon, "High-resolution frequency-wave-number spectrum analysis," *Proc. IEEE*, vol. 57, no. 8, pp. 1408-1418, 1969.
- [4] C. F. Liu and G. S. Liao, "Robust beamforming algorithm using worse-case performance optimization," *Journal of Xidian University (Natural Science)*, vol. 37, no. 1, pp. 1-7, 2010.
- [5] Z. L. Yu, "Robust adaptive beamformers based on worst-case optimization and constraints on magnitude response," *IEEE Transactions on Signal Processing*, vol. 57, no. 7, pp. 2615-2628, 2009.
- [6] J. A. Srar, K. S. Chung, and A. Mansour, "Adaptive array beamforming using a combined LMS-LMS algorithm," *IEEE Transactions on Antennas and Propagation*, vol. 58, no. 11, pp. 3545-3557, 2010.
- [7] S. D. Somasundaram, "Linearly constrained robust Capon beamforming," *IEEE Transactions on Signal Processing*, vol. 60, no. 11, pp. 5845-5856, 2012.
- [8] J. H. Qian, Z. S. He, and T. Liu, "Robust beamforming based on steering vector and covariance matrix estimation," *Circuits, Systems, and Signal Processing*, vol. 37, no. 10, pp. 4665-4682, 2018.
- [9] Z. H. Li, Y. S. Zhang, and H. W. Liu, "A robust STAP method for airborne radar based on clutter covariance matrix reconstruction and steering vector estimation," *Digital Signal Processing*, vol. 78, no. 2, pp. 82-91, 2018.
- [10] F. G. Yan, B. Cao, and J. J. Rong, "Spatial aliasing for efficient direction-of-arrival estimation based on steering vector reconstruction," *EURASIP Journal on Advances in Signal Processing*, vol. 1, p. 121, 2016.
- [11] Y. J. Gu, N. A. Goodman, and S. H. Hong, "Robust adaptive beamforming based on interference

- covariance matrix sparse reconstruction,” *Signal Processing*, vol. 96, no. 5, pp. 375-381, 2014.
- [12] C. W. Zhou, Y. J. Gu, S. He, and Z. Shi, “A robust and efficient algorithm for coprime array adaptive beamforming,” *IEEE Transactions on Vehicular Technology*, vol. 67, no. 2, pp. 1099-1112, 2018.
- [13] Z. Y. Zhang, W. Liu, W. Leng, A. G. Wang, and H. P. Shi, “Interference-plus-noise covariance matrix reconstruction via spatial power spectrum sampling for robust adaptive beamforming,” *IEEE Signal Processing Letters*, vol. 23, no. 1, pp. 121-125, 2016.
- [14] L. Huang, J. Zhang, X. Xu, and Z. F. Ye, “Robust adaptive beamforming with a novel interference-plus-noise covariance matrix reconstruction method,” *IEEE Transactions on Signal Processing*, vol. 63, no. 7, pp. 1643-1650, 2015.
- [15] X. Yuan and L. Gan, “Robust adaptive beamforming via a novel subspace method for interference covariance matrix reconstruction,” *Signal Process*, vol. 130, pp. 233-242, 2017.
- [16] W. X. Li, Z. Yu, Q. B. Ye, and S. Li, “An improved null broadening beamforming method based on covariance matrix reconstruction,” *Applied Computational Electromagnetics Society*, vol. 32, no. 2, pp. 128-134, 2017.
- [17] W. H. Orozco, P. M. Hector, and N. M. Mariko, “A new step-size searching algorithm based on fuzzy logic and neural networks for LMS adaptive beamforming systems,” *Turkish Journal of Electrical Engineering and Computer Sciences*, vol. 24, no. 7, pp. 4322-4338, 2016.
- [18] Z. D. Zaharis, C. Skeberis, and T. D. Xenos, “Design of a novel antenna array beamformer using neural networks trained by modified adaptive dispersion invasive weed optimization based data,” *IEEE Transactions on Broadcasting*, vol. 59, no. 3, pp. 455-460, 2013.
- [19] H. J. Che, C. Li, and X. He, “A recurrent neural network for adaptive beamforming and array correction,” *Neural Networks*, vol. 80, no. C, pp. 110-117, 2016.
- [20] R. Savitha, S. Vigneswaran, and S. Suresh, “Adaptive beamforming using complex-valued radial basis function neural networks,” *TENCON 2009 - 2009 IEEE Region 10 Conference IEEE*, vol. 34, pp. 1-6, 2009.
- [21] A. H. Sallomi and S. Ahmed, “Multi-layer feed forward neural network application in adaptive beamforming of smart antenna system,” *Al-Sadeq International Conference on Multidisciplinary in It and Communication Science and Applications IEEE*, 2016.
- [22] T. Higuchi, K. Kinoshita, and N. Ito, “Frame-by-frame closed-form update for mask-based adaptive MVDR beamforming,” *IEEE International Conference on Acoustics, Speech and Signal Processing (ICASSP)*, 2018.
- [23] J. S. Albus, “A new approach to manipulator control: The cerebellar model articulation controller (CMAC),” *Transactions of the Asme Journal of Dynamic Systems*, vol. 97, no. 3, pp. 220-227, 1975.
- [24] C. C. Chung and C. M. Lin, “Fuzzy brain emotional cerebellar model articulation control system design for multi-input multi-output nonlinear,” *Acta Polytechnica Hungarica*, vol. 12, no. 4, pp. 39-58, 2015.
- [25] C. M. Lin and T. Y. Chen, “Self-organizing CMAC control for a class of MIMO uncertain nonlinear systems,” *IEEE Transactions on Neural Networks*, vol. 20, no. 9, pp. 1377, 2009.
- [26] S. A. Vorobyov, A. B. Gershman, and Z. Q. Luo, “Robust adaptive beamforming using worst-case performance optimization: a solution to the signal mismatch problem,” *IEEE Trans. Signal Processing*, vol. 51, pp. 313-323, Feb. 2003.
- [27] S. Shahbazpanahi, A. B. Gershman, and Z. Q. Luo, “Robust adaptive beamforming for general-rank signal models,” *IEEE Trans. Signal Processing*, vol. 51, pp. 2257-2269, Sept. 2003.
- [28] H. W. Yang, J. G. Huang, and C. Liu, “A modified diagonal loading adaptive beamforming method,” *Computer Simulation*, vol. 27, no. 3, pp. 318-321, 2010.



**Jiaqiang Yu**, a Master candidate at the Shanghai University of Engineering Science, China. He has practiced in Shanghai Baolong Automotive Corporation for one year and he is mainly engaged in the study of automotive millimeter wave radar signal processing algorithm.



**Pingqing Fan**, an Associate Professor works at Shanghai University of Engineering Science, China. She is a Ph.D. candidate of Mechanical Engineering at Shanghai University, China. Her research interests include linear ultrasonic motor design and optimization, micro driver unit of robot and signal processing of millimeter wave radar.